

Revealing Intermolecular Hydrogen Bonding Structure and Dynamics in a Deep Eutectic Pharmaceutical by Magic-Angle Spinning NMR Spectroscopy

Sarah K. Mann, Tran N. Pham, Lisa L. McQueen, Józef R. Lewandowski,* and Steven P. Brown*

Cite This: *Mol. Pharmaceutics* 2020, 17, 622–631

Read Online

ACCESS |



Metrics & More



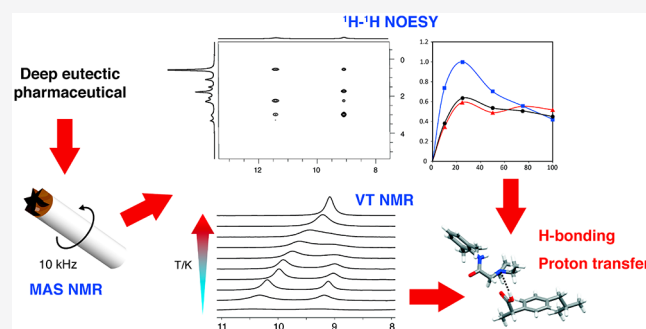
Article Recommendations



Supporting Information

ABSTRACT: Liquid forms of pharmaceuticals (ionic liquids and deep eutectic solvents) offer a number of potential advantages over solid-state drugs; a key question is the role of intermolecular hydrogen bonding interactions in enabling membrane transport. Characterization is challenging since high sample viscosities, typical of liquid pharmaceutical formulations, hamper the use of conventional solution NMR at ambient temperature. Here, we report the application of magic-angle spinning (MAS) NMR spectroscopy to the deep eutectic pharmaceutical, lidocaine ibuprofen. Using variable temperature MAS NMR, the neat system, at a fixed molar ratio, can be studied over a wide range of temperatures, characterized by changing mobility, using a single experimental setup. Specific intermolecular hydrogen bonding interactions are identified by two-dimensional ^1H – ^1H NOESY and ROESY MAS NMR experiments. Hydrogen-bonding dynamics are quantitatively determined by following the chemical exchange process between the labile protons by means of line-width analysis of variable temperature ^1H MAS NMR spectra.

KEYWORDS: NMR spectroscopy, deep eutectics, ionic liquids, hydrogen bonding



INTRODUCTION

As the pharmaceutical industry continues to look for novel ways to improve drug design and enhance delivery, ionic liquids (ILs) have become a promising growth area that seeks to overcome some of the limitations that can exist with solid active pharmaceutical ingredients (APIs).^{1,2} Specifically, API-ILs have shown an ability to markedly improve characteristics such as solubility and permeability, as well as exhibiting the potential for more tolerable routes of administration (transdermal or oral versus injection).^{3–6} In addition to the formation of fully ionized salts, in 2011, Bica et al. demonstrated that hydrogen bonding may drive the “liquefaction” of therapeutics in the form of deep eutectic solvents (DESs), the liquid equivalent of cocrystals.⁷ The nature of the interaction between species is hypothesized to impact the biological behavior of APIs. For example, the membrane permeability of dissociated ions in salt form is limited due to a lack of sufficient lipophilicity. However, API-ILs forming hydrogen bonded complexes should behave more like neutral complexes and transport faster through model membranes compared to dissociated ionic drugs.^{8,9} It is thus very important to characterize both the structure and dynamics of key hydrogen bonding interactions in API-ILs.

While the elucidation of molecular-level structure in liquids is routinely performed using NMR spectroscopy, conventional solution-state (static) NMR can be hindered by sample

viscosity. In these circumstances, slow tumbling can lead to fast transverse relaxation rates and broad spectral lines. ILs and DESs often exhibit high viscosities, typically more than an order of magnitude higher than that of water, and may therefore be difficult to study by NMR in their neat form. While heating viscous liquid samples may address this problem, there are disadvantages such as the disruption of weak intermolecular interactions or even promoting degradation in heat labile samples. In the case of pharmaceuticals, it is more relevant for characterization to occur at temperatures typical of patient use. Magic-angle spinning (MAS) NMR enables, in principle, the study of ILs and DESs over a wide range of temperatures and their characterization in both liquid and solid state in a single setup. There is a very limited number of previous MAS NMR studies on ILs or DESs; these have focused on solutes dissolved in the IL or DES or interactions of the IL or DES with other materials or biological molecules, rather than directly probing intermolecular interactions between the molecules of the neat ILs or DESs themselves. Rencurosi et al. showed that MAS NMR is an effective tool for

Received: October 15, 2019

Revised: December 23, 2019

Accepted: December 30, 2019

Published: December 30, 2019



the study of solutes dissolved in neat IL solvents and for monitoring organic reactions in neat ILs.¹⁰ Other applications of MAS NMR associated with ILs include peptide- and protein-IL interactions^{11,12} and the study of surface-immobilized ILs important for catalysis.¹³

This study considers the prototype deep eutectic “liquid cocrystal”^{7,14} formed between the pain relieving compounds lidocaine and ibuprofen,^{8,15} denoted Lid-Ibu (Figure 1a). The

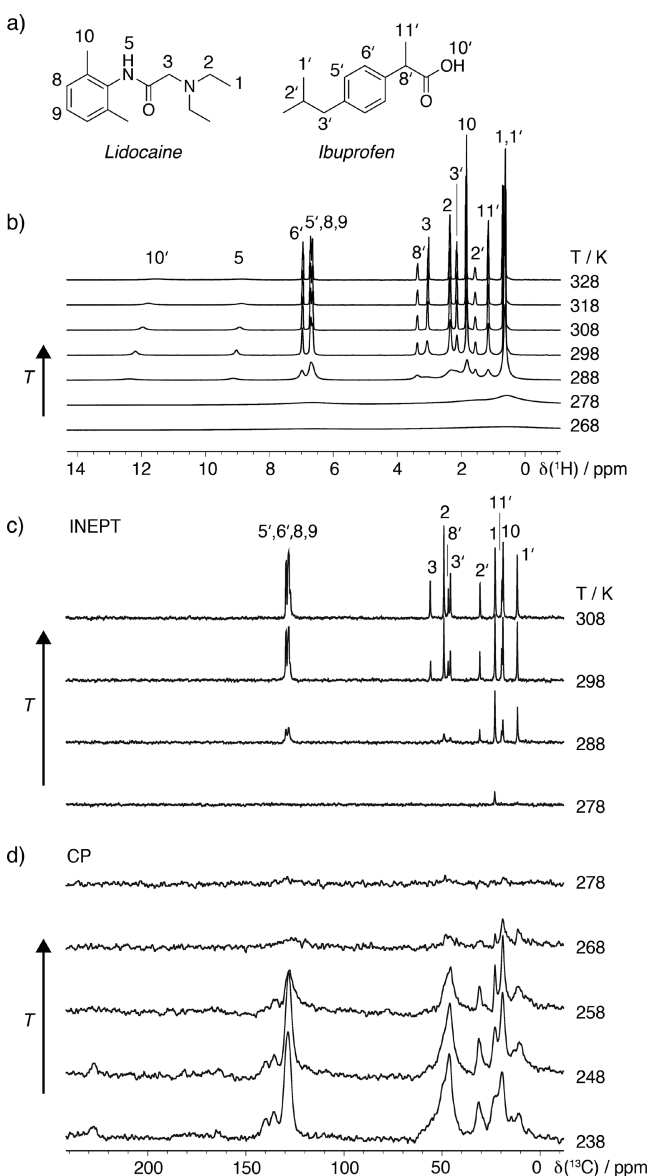


Figure 1. Variable-temperature MAS ($\nu_{\text{OH}} = 500$ MHz, $\nu_r = 12.5$ kHz) NMR spectra of Lid-Ibu, see chemical structures of lidocaine and ibuprofen in panel a: (b) one-pulse ^1H , (c, d) ^{13}C with (c) refocused INEPT or (d) CP transfer from ^1H .

neutral forms of lidocaine and ibuprofen are solids at room temperature, with melting points (T_m) of 68–69 °C¹⁶ and 75–77 °C,¹⁶ respectively, while the 1:1 combination, Lid-Ibu, is liquid at room temperature with a glass transition temperature of –27 °C.⁸ Wang et al. demonstrated via spectroscopic analysis that it is the COO–H...N (tertiary amine) hydrogen bond interaction rather than proton transfer that reduces the T_m ; Lid-Ibu is a poorly ionized, hydrogen-bonded DES,⁸ in contrast to a true API-IL (completely ionized) as it has been

defined in some publications.¹⁷ The hydrogen bonding between the two APIs has been shown to promote membrane transport; neat Lid-Ibu transported faster through a model silicone membrane compared to the commercial salt forms of the APIs,⁸ and transdermal administration of Lid-Ibu to rats resulted in faster and higher systemic absorption of lidocaine compared to the commercial salt [Lid]Cl.¹⁸ These studies suggest that strong hydrogen bond interactions between lidocaine and ibuprofen in the deep eutectic cocrystal form might be advantageous for transdermal drug delivery.

With the pharmaceutical application of such complexes in mind, our particular focus is the identification of intermolecular hydrogen bonding interactions and the quantitative characterization of dynamic chemical exchange associated with the making and breaking of hydrogen bonding between the two components. This is enabled by the unique possibility afforded by MAS NMR spectroscopy to characterize a single complex, that is, with a fixed molar ratio, over a wide range of temperatures.

EXPERIMENTAL SECTION

Sample Preparation. Lidocaine and ibuprofen were purchased from Sigma-Aldrich (Gillingham, UK) and used as received. Lidocaine ibuprofen was prepared by stirring an equal molar ratio of lidocaine and ibuprofen together in an oil bath at 100 °C for 1 h. The mixture was then stored in a vacuum oven at 50 °C for 24 h, after which the sample was stored at room temperature. Lid-Ibu is a pale-yellow liquid at room temperature.

MAS NMR. MAS NMR experiments were performed at ^1H Larmor frequencies of $\nu_{\text{OH}} = 500$ (11.7 T), $\nu_{\text{OH}} = 600$ (14.1 T), and $\nu_{\text{OH}} = 850$ (20.0 T) MHz using Bruker Avance III (500 and 850 MHz) and II+ (600 MHz) spectrometers. All experiments were performed using either a 4 mm triple-resonance MAS probe operating in double-resonance mode or using a Bruker 4 mm E^{free} probe ($\nu_{\text{OH}} = 500$ MHz). The E^{free} probe utilizes a low inductance proton RF coil to minimize RF sample heating by reducing the E-field. In all experiments, the ^1H 90° pulse was of duration 2.5 μs (corresponding to a nutation frequency, $\nu_1 = 100$ kHz) except experiments run using the E^{free} probe, where the ^1H 90° pulse length was 3.5 μs ($\nu_1 = 71$ kHz). Except where otherwise stated, a spinning frequency of 10 or 12.5 kHz was used, and reported temperatures are the gas input temperature.

^1H One-Pulse MAS NMR. One-dimensional ^1H spectra were recorded with a recycle delay of 2 s and 4 coadded transients. We note that the changes observed in the ^1H spectra over time (~ 2 ppm shift for the carboxylic acid proton) only occurred for Lid-Ibu stored at room temperature in a glass vial and repacked at a later date, whereas only minor shifts (~ 0.2 ppm) occurred for the sample stored in the MAS rotor, likely due to lower exposure to humidity.

^1H – ^{13}C CP MAS and ^1H – ^{13}C Refocused INEPT. In order to collect NMR spectra for the lower natural abundance ^{13}C nuclei, scalar or dipolar coupling based methods to transfer magnetization from ^1H to ^{13}C are commonly employed depending on the nature of the sample and the required information. In solution NMR, the INEPT technique using through-bond scalar couplings is used for most heteronuclear correlation experiments. Solid-state NMR of dilute nuclei such as ^{13}C spectra is typically achieved using cross-polarization (CP), which uses through-space dipolar interactions. A very viscous IL or DES can be considered to lie somewhere on a

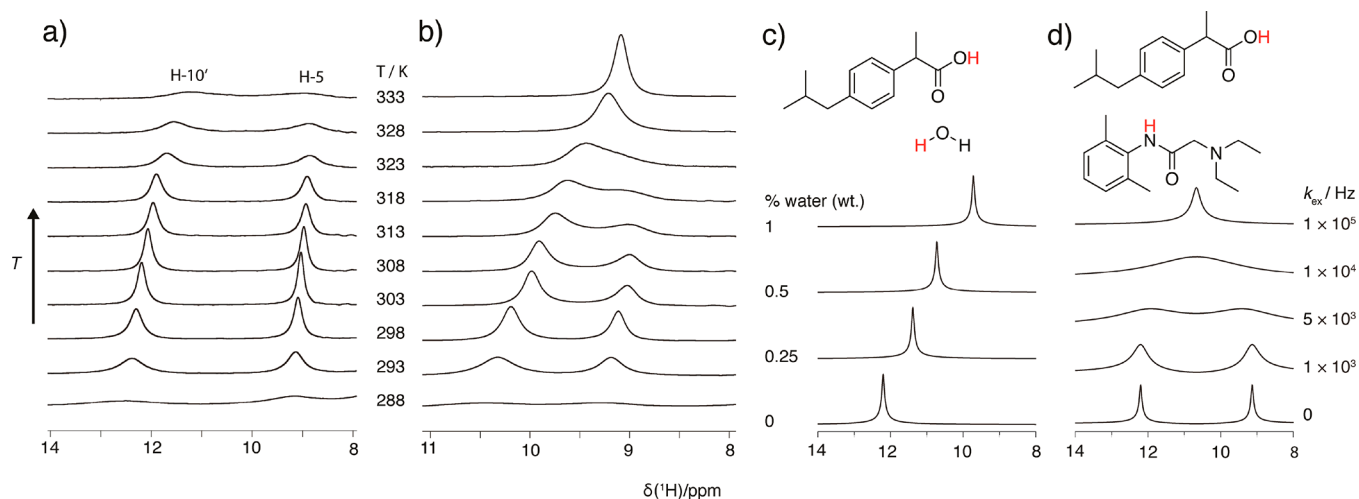


Figure 2. (a, b) Effect of temperature on the high-ppm region of ¹H MAS NMR spectra ($\nu_{\text{OH}} = 500$ MHz, $\nu_r = 12.5$ kHz) of Lid-Ibu in (a) a freshly prepared sample and (b) a sample stored at room temperature for approximately eight months. (c, d) Numerical simulations (see equations S7–S9 in section S5) of the effect of chemical exchange for the two processes: (c) fast exchange of the carboxylic acid proton with varying amounts of water and (d) exchange between the carboxylic acid and amide protons.

continuum between liquid and solid. The feasibility of CP or INEPT techniques is likely to depend on its position on this continuum, which dictates dephasing times and the strength of residual dipolar couplings, factors that affect the efficiency of magnetization transfer for these two methods. This can be clearly seen in the variable temperature ¹H–¹³C refocused INEPT and CP ¹³C MAS NMR spectra presented in this paper.

¹H–¹³C cross-polarization (CP) and refocused INEPT spectra were acquired at $\nu_{\text{OH}} = 500$ MHz and $\nu_r = 12.5$ kHz MAS frequency; 128 transients were coadded, and a recycle delay of 1.5 s was used. Cross-polarization was achieved using a 70% to 100% ramp¹⁹ on the ¹H channel for a contact time of 500 μ s. The ¹H and ¹³C nutation frequencies were 60 and 47.5 kHz, respectively. The refocused INEPT spectra were acquired with a spin–echo ($\frac{\tau}{2} - \pi - \frac{\tau}{2}$) duration of $\tau = 2$ ms. In ¹³C detected experiments, SPINAL-64²⁰ ¹H heteronuclear decoupling was applied during acquisition at a nutation frequency of 88 kHz (CP) or 13 kHz (INEPT) and a pulse duration of 5.4 μ s (CP) or 38 μ s (INEPT).

¹H–¹H NOESY and ROESY. NOESY ($\nu_{\text{OH}} = 600$ MHz) and ROESY ($\nu_{\text{OH}} = 500$ MHz) spectra were recorded with 8 transients coadded for each of 512 t_1 FIDs, using the States-TPPI²¹ method to restore sign discrimination in the F_1 dimension with a t_1 increment of 80 μ s. NOESY mixing times between 3 and 100 ms and a recycle delay of 4 s were used, corresponding to an experimental time of approximately 4.5 h. A ROESY spectrum was recorded with a mixing time of 10 ms during which a spin lock of ~ 20 kHz was applied and a recycle delay of 2 s, corresponding to an experimental time of 2.5 h. NOESY ($\nu_{\text{OH}} = 850$ MHz) spectra were recorded with 4 transients coadded for each of 512 t_1 FIDs, using the States-TPPI²¹ method to restore sign discrimination in the F_1 dimension with a t_1 increment of 59 μ s and a recycle delay of 3 s, corresponding to an experimental time of 3.5 h. An eight-step nested phase cycle was used in the NOESY experiments ($\nu_{\text{OH}} = 600$ MHz) where the three ¹H 90° pulses were cycled through phases (i) $x - x$, (ii) $x x - x - x$, and (iii) $x x x x - x - x - x - x$ and the receiver was cycled through phases $x - x - x x - x x x - x$. A four-step nested phase cycle was used

in the NOESY experiments ($\nu_{\text{OH}} = 850$ MHz) where the three ¹H 90° pulses were cycled through phases (i) $x - x$, (ii) x , and (iii) $x x - x - x$ and the receiver was cycled through phases $x - x - x x$. An eight-step phase cycle was used in the ROESY experiment where the two ¹H 90° pulses before and after the spin-lock were cycled through phases $x - x - x x y - y - y y$ and $x - x x - x y - y y - y$ and the receiver was cycled through phases $x - x - x x y - y - y y$.

¹H and ¹³C chemical shifts are referenced to TMS at 0 ppm using L-alanine as a secondary reference (1.1 ppm for the lower ppm ¹H resonance and 177.8 ppm for the higher ppm ¹³C resonance), corresponding to adamantane at 1.85 ppm (¹H)²² and 38.5 ppm (¹³C).²³ For all ¹H VT spectra, the chemical shift axis is referenced such that the methyl (H-11') chemical shift is unchanged from the value at 298 K (1.15 ppm).

RESULTS AND DISCUSSION

¹H MAS NMR spectra of neat Lid-Ibu obtained for temperatures between 268 and 328 K are shown in Figure 1b. As with conventional liquids, the viscosity of ILs and DESs are expected to be strongly temperature dependent, the effect of which is observed in the broadening of the NMR spectra at lower temperatures. At ambient temperature, 10 kHz MAS is sufficient to resolve all proton resonances of Lid-Ibu, apart from overlap in the aromatic region and for the methyl groups (H-1 and H-1') while ensuring that spinning sidebands lie outside the chemical shift range in the ¹H spectra (Figure S1). Figure 1c,d compares ¹³C spectra recorded using refocused INEPT and CP, respectively. The INEPT spectra show increased sensitivity at higher temperatures when the sample is “more liquid”; however at room temperature and below, there is very little signal, attributable to the rapid dephasing of transverse proton magnetization in the higher viscosity sample. While CP is efficient at low temperatures in “solid-like” samples, the efficacy decays upon heating as dipolar couplings are partially averaged by molecular motion. Our observation matches that of Sarkar et al., who reported CP transfers in a high viscosity natural DES (glucose/choline chloride/water in a 1:1:4 ratio) with increasing transfer efficiency upon a decrease in temperature.²⁴ Overall, the result is a region

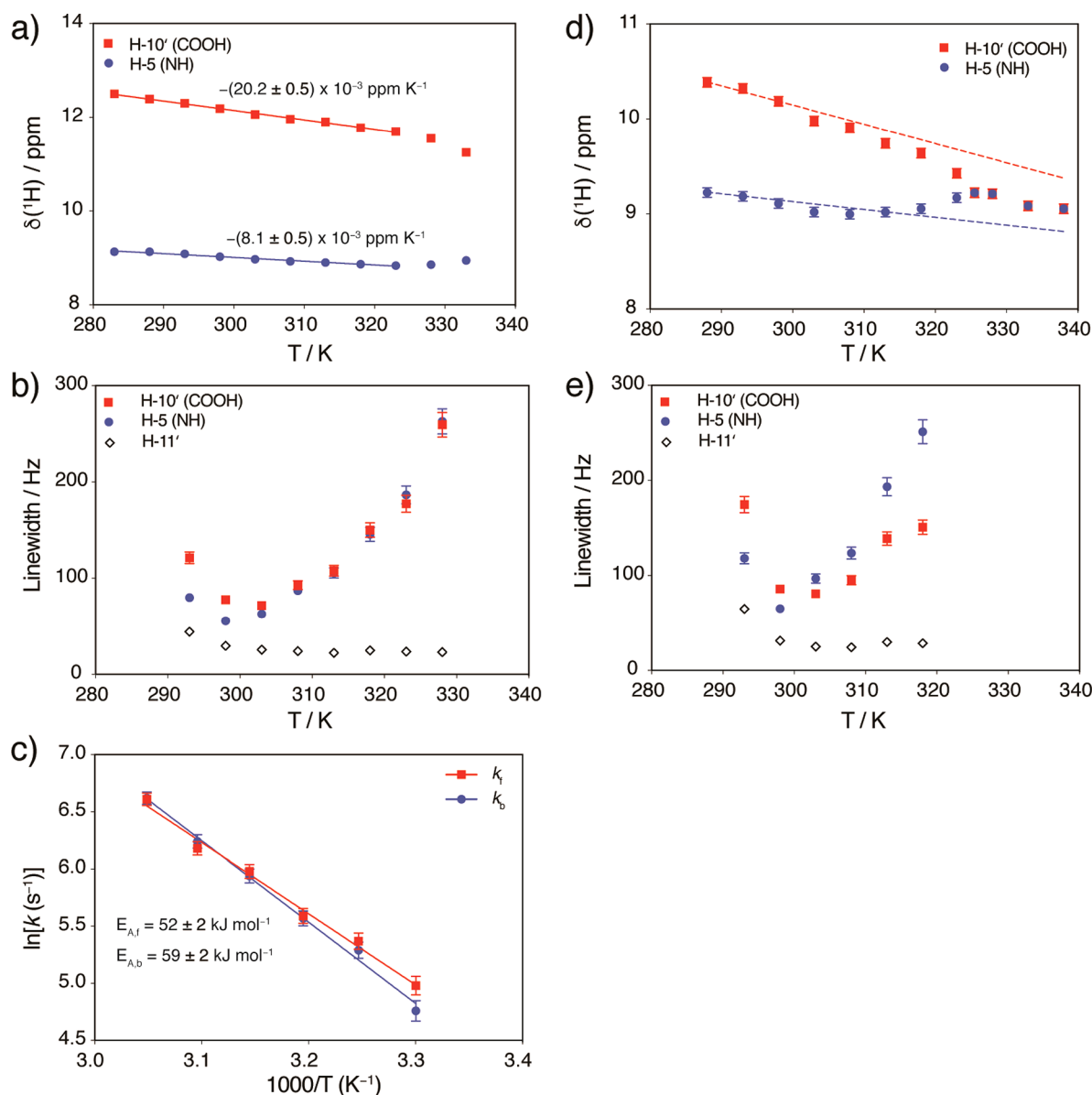


Figure 3. Analysis of chemical exchange process between H-10' and H-5 of Lid-Ibu in (a, b, c) a freshly prepared sample and (d, e) a sample stored at room temperature for approximately eight months: The effect of temperature on (a, d) the observed chemical shift and (b, e) the line width (full width at half-maximum height) in ¹H one-pulse MAS NMR spectra (Figure 2a,b). In panel a, the best-fit straight lines in the slow exchange regime obtained from a linear regression analysis used to determine the rate of change of the chemical shift with respect to temperature are shown. The dashed lines in panel d show the same temperature dependence of the chemical shift as in panel a for comparison. (c) Arrhenius plots for the proton exchange process. The rate constants, k_f and k_b , were obtained from the line width analysis carried out for the 1D ¹H one-pulse VT MAS NMR spectra (Figure 2a; see discussion on chemical exchange in section S5 for further details). The best-fit straight lines obtained from a linear regression analysis are shown. The estimated error in the measured chemical shift (a, d) and line width (b, e) of ± 0.05 ppm and 5%, respectively, are not shown if smaller than the symbol height.

between liquid and solid phases (between 268 and 288 K for the case of Lid-Ibu) in which the transfer of coherences from the ¹H to ¹³C by either technique is inefficient.

Inspection of the 1D proton spectra as a function of temperature reveals that while the chemical shifts of the CH protons are essentially unchanged, there are changes for the NH and COOH protons, which can be attributed to different interactions and chemical exchange processes. Figure 2a presents the region between 8.0 and 14 ppm of the variable temperature (VT) 1D proton spectra. The carboxylic acid (H-10') and amine (H-5) resonances gradually shift to lower ppm values with increasing temperature, with the effect being more

prominent for the COOH proton (Figure 3a). Such temperature dependent changes in ¹H chemical shifts have previously been reported for protons participating in hydrogen bonds for both liquids^{25–29} and solids.^{30–32}

We also note that the carboxylic acid resonance (H-10') shifted to lower ppm over time (over a period of months) from 12.2 ppm to as low as 10.2 ppm at 298 K (Figures 2a,b and S2). ILs and DESs are generally hygroscopic and readily absorb water from the environment. The shift in the COOH peak can be accounted for by the absorption of a small amount of water in fast exchange with the carboxylic acid proton. In fast chemical exchange between two sites, a single population-

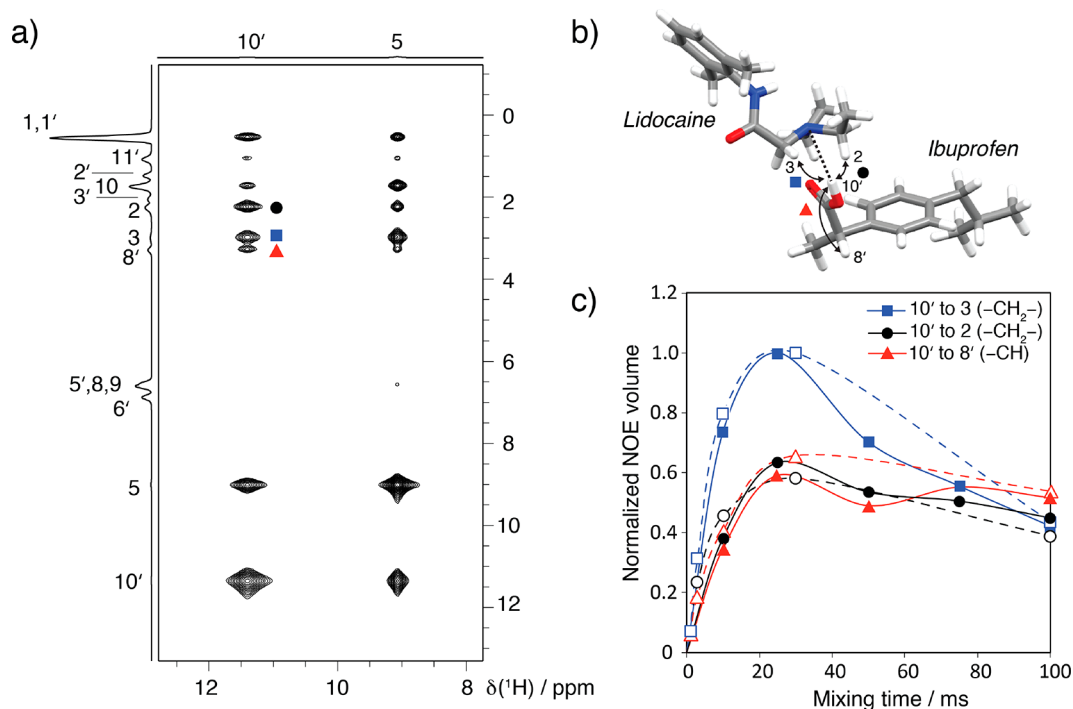


Figure 4. ^1H - ^1H NOESY MAS ($\nu_r = 10$ kHz) NMR of Lid-Ibu with input gas at 298 K: (a) An expanded region of a 2D spectrum ($\nu_{\text{OH}} = 600$ MHz) with skyline projections for $\tau_{\text{mix}} = 10$ ms. The base contour level is at 0.03% of the maximum peak intensity. (b) Proposed hydrogen-bonded structure accounting for the strong intermolecular NOEs (H-10' to H-2 and H-3) as shown by arrows. (c) Comparison of NOE build-up curves at $\nu_{\text{OH}} = 600$ MHz (solid lines, filled symbols) and $\nu_{\text{OH}} = 850$ MHz (dashed lines, open symbols) for the carboxylic acid proton (H-10') to H-3 (blue squares), H-2 (black circles), and H-8' (red triangles). The H-10' to H-8' NOE is an intramolecular contact between protons of ibuprofen (see panel b) and is shown for comparison to the intermolecular contacts between the lidocaine and ibuprofen (H-10' to H-3 and H-2). To interpret the NOESY spectra, the cross-peak integrals were corrected for the number of equivalent protons contributing to the observed NOE signal by dividing by the product of the number of each proton, $n_A n_B$, and then normalized to the maximum signal for the H-10' to H-3 cross peak at a mixing time of 10 ms. Lines are included as guides for the eye. The integration error is estimated to be $<2\%$ and is smaller than the symbol height. The full 2D spectrum and rows extracted for H-10' (COOH) and H-5 (NH) are presented in Figures 6a and S3, while Figure S4 presents all NOE build-up curves for H-10' at $\nu_{\text{OH}} = 600$ MHz.

weighted average shift ($\delta^{\text{obs}} = p_{\text{COOH}}\delta_{\text{COOH}} + p_{\text{H}_2\text{O}}\delta_{\text{H}_2\text{O}}$) is observed. Less than 1% water (by mass) could result in changes of greater than 2 ppm (Figure 2c). This leads to the important point that the absence of a peak at the expected chemical shift of water (approximately 4.7 ppm) does not necessarily indicate that the sample is dry. From the observed change in the COOH chemical shift, the approximate water content can be calculated (assuming the chemical shift in the absence of exchange, $\delta_{\text{COOH}} = 12.2$ ppm, that is, the chemical shift at 298 K observed directly after preparation and drying of Lid-Ibu, and $\delta_{\text{H}_2\text{O}} = 4.7$ ppm) to be 0.74 wt % H_2O , corresponding to 1 equiv of H_2O per 5.5 Lid-Ibu, after a period of eight months of storage at ambient conditions. The presence of water in API-DESS or -ILs can be expected to influence the properties. Similarly, the presence of water in crystalline hydrates is known to dramatically alter the physicochemical properties of pharmaceuticals compared to their anhydrous forms.^{33,34} The environment of water molecules and the role of hydrogen bonding in solid pharmaceutical hydrates has been characterized by fast (>60 kHz) ^1H MAS solid-state NMR.^{35,36} The environment of water in API-ILs or -DESS, such as Lid-Ibu, could be characterized by further MAS NMR studies.

A second exchange process between the carboxylic acid and amide proton is evident with significant broadening of the peaks with increasing temperature (Figure 2a,b). This is more obvious in the sample with higher water content, where, within the temperature range studied, the peaks first broaden and

then merge into a single peak (Figure 2b). This is consistent with a two-site chemical exchange process where the appearance of the NMR spectra depends on the relative magnitudes of the rate constant, k_{ex} and the frequency difference between the two exchanging resonances, $\Delta\nu$ (both in s^{-1}). The two peaks initially broaden and approach one another in the slow ($k_{\text{ex}} \ll \Delta\nu$) to intermediate exchange regime ($k_{\text{ex}} \approx \Delta\nu$) before merging into a single peak at the point of coalescence (corresponding to $k_{\text{ex}} = \pi\Delta\nu/\sqrt{2}$) and then narrowing in the fast exchange limit ($k_{\text{ex}} \gg \Delta\nu$) (Figure 2d). We note that the exchange may also be mediated by a small population of water; this would be expected to show similar line shapes to a direct exchange process.

The changes in chemical shift and line width for the exchanging proton peaks are shown graphically in Figure 3. In the slow exchange regime, k_{ex} may be obtained from analysis of the line widths of the exchanging peaks (see section S5 for further details). At temperatures below 298 K, additional line broadening of all resonances was observed due to slower transverse relaxation with increased sample viscosity and an accurate value of the line width in the absence of exchange could not be obtained for the H-10' or H-5 resonances (Figure 3b,e). Since all other peaks not involved in exchange showed comparable line widths, we therefore took the line width of the well resolved methyl peak H-11' as a reference to obtain an approximate value of the line widths in the absence of exchange. The broadening of the exchanging peaks was taken

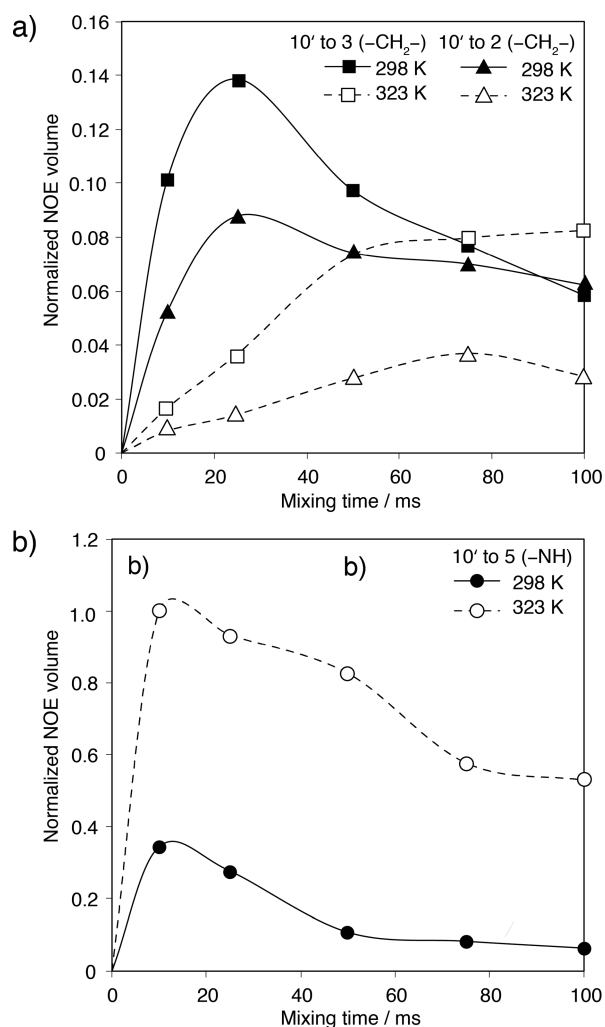


Figure 5. (a, b) ^1H NOESY MAS ($\nu_r = 10$ kHz) NMR build-up curves ($\nu_{\text{OH}} = 600$ MHz) for the carboxylic acid proton (H-10'; 11.4 ppm) of Lid-Ibu to (a) H-3 (squares) and H-2 (triangles) and (b) H-5 (circles) recorded at 298 K (solid lines, filled symbols) and 323 K (dashed lines, open symbols). The integration error is estimated to be $<2\%$ and is smaller than the symbol height.

as the difference between the observed line width and the width of the reference peak at each temperature. The rate constant of the forward and reverse reactions, k , is then given by this value multiplied by π . In Figure 3c, $\ln k$ (k_f or k_b) versus the inverse temperature is plotted between 303 and 328 K. A linear fit (with R^2 values of 0.99) produced activation energies of 52 ± 2 kJ mol $^{-1}$ and 59 ± 2 kJ mol $^{-1}$ for the forward and reverse reactions, respectively, from the Arrhenius equation, $\ln(k) = \ln(a) - E_a/(RT)$. These values are similar to activation energies of 30–90 kJ mol $^{-1}$ frequently reported for chemical exchange processes studied by NMR.^{31,37,38} Over the temperature range studied, the carboxylic acid and amide protons are in slow exchange, with only a small exchange-induced chemical shift of the peaks observed above 318 K (Figures 2a, 3a). However, in a sample of Lid-Ibu with higher water content, the two peaks are at ppm values significantly closer together and the chemical exchange therefore appears faster on the chemical shift time-scale (Figures 2b, 3d). The peaks initially broaden with increasing temperature and coalesce at ~ 325 K. At higher temperatures, significant narrowing of the peak indicates exchange in the intermediate-fast exchange regime.

While the ^1H NMR chemical shift is a powerful probe of intermolecular interactions, particularly hydrogen bonding, 2D correlation experiments are useful for identifying pairs of nuclei involved in such interactions. In nuclear Overhauser effect spectroscopy (NOESY) experiments, magnetization is transferred through space during the mixing time, permitting the study of intermolecular interactions. ^1H – ^1H MAS-NOESY experiments have previously been used to detect intermolecular hydrogen bonding between solvent molecules and a DES³⁹ and between a drug and polymer excipient in supersaturated solution.⁴⁰ In addition to MAS-NOESY experiments, a variant where the application of radio frequency-driven recoupling (RFDR)⁴¹ during the NOESY mixing time reintroduces the homonuclear dipolar couplings under MAS has been described to enhance the coherent ^1H – ^1H dipolar coupling-driven transfer and has been applied to investigate membrane interactions of peptides and proteins.^{42,43} In liquids, cross-relaxation (the NOE) induced by modulation of dipolar couplings by molecular motions is responsible for the transfer of magnetization between pairs of nuclei spins close in space (typically within ~ 5 Å). In the solid state, the same pulse sequence is often referred to as a spin diffusion experiment because the dominant mechanism responsible for the transportation of magnetization is spin diffusion, which is not related to molecular motion but rather is a coherent effect originating from an incomplete averaging by MAS of the ^1H – ^1H dipolar interactions.^{44,45} Note that the term spin diffusion is used differently in solution NMR and refers to an incoherent multistep NOE process. To avoid confusion, the two definitions of spin diffusion will be referred to as coherent spin diffusion (solids) and incoherent spin diffusion (liquids). In samples on the continuum from liquid to solid, both the NOE and coherent spin diffusion are expected to contribute to the NOESY spectra. In the following discussion, we interpret the presented NOESY data in terms of the NOE effect for Lid-Ibu, that is, reflecting a state that lies closer to the liquid regime at room temperature and above.

A section of a two-dimensional ^1H – ^1H NOESY MAS spectrum is shown in Figure 4a. All NOEs are the same sign as the diagonal as expected for viscous liquids with slow molecular tumbling. Specific interactions between lidocaine and ibuprofen protons were observed particularly from the carboxylic acid proton (H-10') of ibuprofen. Three strong cross peaks to lidocaine are observed, which can be attributed to strong intermolecular contacts (to protons adjacent to the tertiary nitrogen H-2 and H-3) or chemical exchange (to the amide proton H-5). The NOEs to H-2 and H-3 likely result from a hydrogen bond between the carboxylic acid proton and tertiary amine nitrogen as shown in Figure 4b. Selected NOE build-up curves for H-10' are plotted in Figure 4c. NOE volumes are shown per proton contributing to the cross peak and normalized to the maximum NOE volume. As expected, an intramolecular NOE is also observed to the adjacent proton (H-8'). While intramolecular NOE signals are known to show an r^{-6} distance dependence, the intermolecular NOE is much more complicated and may vary between the typical r^{-6} short-range behavior to r^{-1} long-range behavior depending on the spectrometer frequency.⁴⁶ We therefore performed NOE experiments at two frequencies (600 and 850 MHz). Build-up curves of NOEs from the carboxylic acid proton (H-10') showed the same trends at both magnetic field strengths (Figure 4c), with the strongest NOEs belonging to H-2 and H-3 of lidocaine (intermolecular), followed by intramolecular H-

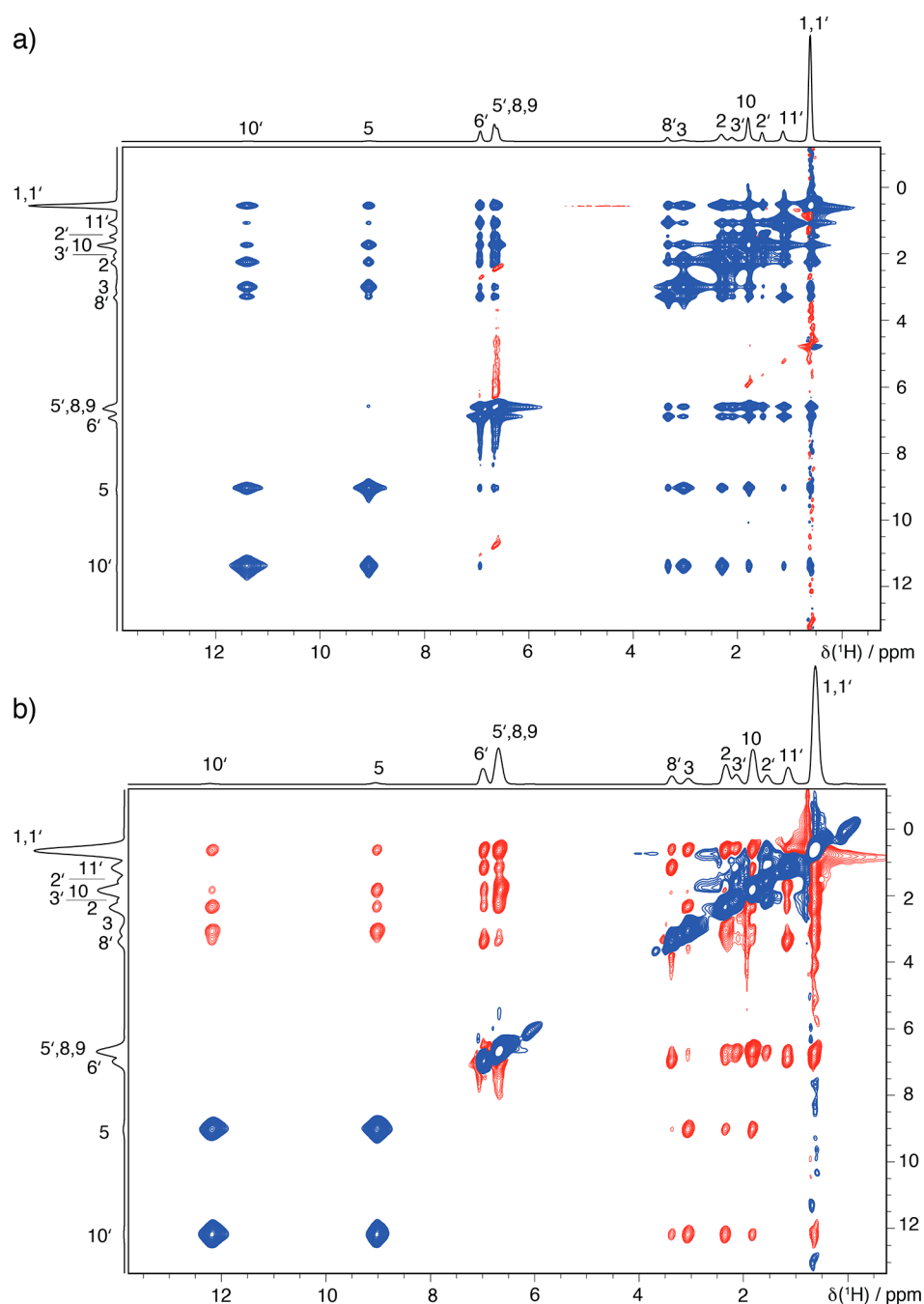


Figure 6. (a) ^1H – ^1H NOESY MAS NMR spectrum ($\nu_{\text{OH}} = 600$ MHz, $\nu_r = 10$ kHz, 298 K) and (b) ^1H – ^1H ROESY MAS NMR spectrum ($\nu_{\text{OH}} = 500$ MHz, $\nu_r = 10$ kHz, 298 K) with skyline projections of neat Lid-Ibu recorded using a mixing time (NOESY) or spin-lock (ROESY) of duration 10 ms. Positively phased peaks are shown in blue, and negative peaks are shown in red. The base contour level is at 0.03% (a) and 0.05% (b) of the maximum peak intensity.

$8'$, indicating a dominant short-range (r^{-6}) behavior. Note that the rapid build-up and decay of the NOE indicates the need for short mixing times in viscous samples. While mixing times greater than 200 ms are common for acquiring NOESY spectra of small molecules in solution, at mixing times greater than 50 ms in slow-tumbling neat Lid-Ibu all protons show similar contacts to all other protons due to incoherent spin-diffusion.⁴⁷ In previous liquid-state NMR data published on neat Lid-Ibu performed at 70 °C under static conditions, hydrogen-bonding was indirectly evidenced by observing shifts to higher ppm of the protons adjacent to the tertiary nitrogen in lidocaine (H-2, H-3) with increasing ibuprofen content.⁸ Under MAS, we are

able to directly detect this hydrogen bond at ambient temperature in a single sample (the 1:1 molar ratio Lid-Ibu). We note that at the time of recording the NOESY spectra, the sample had absorbed approximately 0.24 wt % H_2O (based on the observed COOH chemical shift of 11.4 ppm), corresponding to one equivalent of H_2O per 17 Lid-Ibu. While this small amount of water can be expected to participate in hydrogen bonding to the lidocaine and ibuprofen, the dominant hydrogen bond interaction is between the two APIs.

Figure 5 shows intermolecular NOE build-up curves recorded at two temperatures (298 and 323 K) for the carboxylic acid proton of ibuprofen (H-10') to the protons

adjacent to the tertiary nitrogen (H-2 and H-3, Figure 5a) and the amide proton (H-5, Figure 5b) of lidocaine. As a sample is heated, it would be expected that reduced NOESY cross peaks would result from faster motion, as the NOE enhancement decreases as it approaches a zero crossing, and may be further reduced by weakening of intermolecular interactions in the sample. In contrast to all other cross peaks to H-10', which showed decreased intensity at higher temperature (Figure 5a), the amide (H-5) to acid cross peak is stronger at 323 K (Figure 5b). This behavior is consistent with the VT 1D spectra (see Figure 2), which indicate exchange between the amide and acid protons, and is confirmed by rotating-frame NOE spectroscopy (ROESY) spectra where the exchange-induced cross peaks appear with opposite intensity compared to cross peaks originating from the NOE mechanism (Figure 6). The increased intensity of the 10' to 5 NOESY cross peak at 323 K (Figure 5b) is consistent with the increase of the chemical exchange rate as the sample is heated (see previous discussion of Figures 2 and 3).

In conclusion, MAS NMR spectroscopy has been applied to probe specific hydrogen interactions and their dynamics via chemical exchange in a DES. A key advantage of utilizing MAS is the ability to study the system over a wide temperature range. This is to be compared with the solution-state NMR analysis of Wang et al. that could only be performed at 70 °C and required an analysis of a series of samples composed of varying molar ratios of lidocaine and ibuprofen to make inferences about the hydrogen bonding interactions.⁸

Using 10 kHz MAS, the resolution of the carboxylic acid and amide protons is sufficient to allow analysis of dynamic chemical exchange processes and yield 2D NOESY and ROESY spectra that allow the direct probing of the important hydrogen bond interactions. When seeking to develop a molecular pharmaceutical for medical application, a detailed understanding of such interactions between the components of ILs or DESs is a prerequisite for an understanding of the biological behavior. Specifically, for Lid-Ibu, strong hydrogen bond interactions have been hypothesized to account for promising transport rates of the APIs through model membranes.⁸ With growing interest in ILs and DESs as new formulations for improved therapeutics, we believe that MAS NMR will prove to be indispensable for their characterization, complementing the application of solid-state NMR to conventional solid pharmaceuticals.^{48,49}

■ ASSOCIATED CONTENT

SI Supporting Information

The Supporting Information is available free of charge at <https://pubs.acs.org/doi/10.1021/acs.molpharmaceut.9b01075>.

Effect of MAS frequency on ¹H NMR spectra, ¹H MAS NMR spectra for comparison of changes over time, rows extracted from NOESY spectra, NOESY build up curves for H-10' to all other protons, and analysis of chemical exchange (PDF)

■ AUTHOR INFORMATION

Corresponding Authors

Józef R. Lewandowski – University of Warwick, Coventry, U.K.; orcid.org/0000-0001-6525-7083; Email: J.R.Lewandowski@warwick.ac.uk

Steven P. Brown – University of Warwick, Coventry, U.K.; orcid.org/0000-0003-2069-8496; Email: S.P.Brown@warwick.ac.uk

Other Authors

Sarah K. Mann – University of Warwick, Coventry, U.K.
Tran N. Pham – GSK R&D, Stevenage, U.K.
Lisa L. McQueen – GSK R&D, Collegeville, Pennsylvania

Complete contact information is available at: <https://pubs.acs.org/10.1021/acs.molpharmaceut.9b01075>

Notes

The authors declare no competing financial interest. The data for this study is provided as a supporting data set from WRAP, the Warwick Research Archive Portal at <http://wrap.warwick.ac.uk/131708>.

■ ACKNOWLEDGMENTS

This work was partially funded by GSK. S.K.M. is supported by a University of Warwick International Chancellor's scholarship. The UK 850 MHz solid-state NMR Facility used in this research was funded by EPSRC and BBSRC, as well as the University of Warwick including via partial funding through Birmingham Science City Advanced Materials Projects 1 and 2 supported by Advantage West Midlands and the European Regional Development Fund. We thank Dinu Iuga for experimental assistance. J.R.L. acknowledges funding from ERC Starting Grant 639907 and BBSRC grant BB/R010218/1. Andy Edwards, Bernie O'Hare, Lyndsey Knight, and Dewey Barich (GSK) are thanked for discussions of the NMR results.

■ REFERENCES

- (1) Shamshina, J. L.; Berton, P.; Wang, H.; Zhou, X.; Gurau, G.; Rogers, R. D. Ionic Liquids in Pharmaceutical Industry. *Green Techniques for Organic Synthesis and Medicinal Chemistry*; Wiley-Blackwell: 2018.
- (2) Martins, I. C. B.; Oliveira, M. C.; Diogo, H. P.; Branco, L. C.; Duarte, M. T. MechanoAPI-ILs: Pharmaceutical Ionic Liquids Obtained through Mechanochemical Synthesis. *ChemSusChem* **2017**, *10* (7), 1360–1363.
- (3) Hough, W. L.; Rogers, R. D. Ionic Liquids Then and Now: From Solvents to Materials to Active Pharmaceutical Ingredients. *Bull. Chem. Soc. Jpn.* **2007**, *80* (12), 2262–2269.
- (4) Egorova, K. S.; Gordeev, E. G.; Ananikov, V. P. Biological Activity of Ionic Liquids and Their Application in Pharmaceuticals and Medicine. *Chem. Rev.* **2017**, *117* (10), 7132–7189.
- (5) Sahbaz, Y.; Williams, H. D.; Nguyen, T.-H.; Saunders, J.; Ford, L.; Charman, S. A.; Scammells, P. J.; Porter, C. J. H. Transformation of Poorly Water-Soluble Drugs into Lipophilic Ionic Liquids Enhances Oral Drug Exposure from Lipid Based Formulations. *Mol. Pharmaceutics* **2015**, *12* (6), 1980–1991.
- (6) Shamshina, J. L.; Cojocaru, O. A.; Kelley, S. P.; Bica, K.; Wallace, S. P.; Gurau, G.; Rogers, R. D. Acyclovir as an Ionic Liquid Cation or Anion Can Improve Aqueous Solubility. *ACS Omega* **2017**, *2* (7), 3483–3493.
- (7) Bica, K.; Shamshina, J.; Hough, W. L.; MacFarlane, D. R.; Rogers, R. D. Liquid forms of pharmaceutical co-crystals: exploring the boundaries of salt formation. *Chem. Commun.* **2011**, *47* (8), 2267–2269.
- (8) Wang, H.; Gurau, G.; Shamshina, J.; Cojocaru, O. A.; Janikowski, J.; MacFarlane, D. R.; Davis, J. H.; Rogers, R. D. Simultaneous membrane transport of two active pharmaceutical ingredients by charge assisted hydrogen bond complex formation. *Chem. Sci.* **2014**, *5* (9), 3449–3456.

- (9) Stoimenovski, J.; MacFarlane, D. R. Enhanced membrane transport of pharmaceutically active protic ionic liquids. *Chem. Commun.* **2011**, 47 (41), 11429–11431.
- (10) Rencurosi, A.; Lay, L.; Russo, G.; Prosperi, D.; Poletti, L.; Caneva, E. HRMAS NMR analysis in neat ionic liquids: a powerful tool to investigate complex organic molecules and monitor chemical reactions. *Green Chem.* **2007**, 9 (3), 216–218.
- (11) Mrestani-Klaus, C.; Richardt, A.; Wespe, C.; Stark, A.; Humpfer, E.; Bordusa, F. Structural Studies on Ionic Liquid/Water/Peptide Systems by HR-MAS NMR Spectroscopy. *ChemPhysChem* **2012**, 13 (7), 1836–1844.
- (12) Warner, L.; Gjersing, E.; Follett, S. E.; Elliott, K. W.; Dzyuba, S. V.; Varga, K. The effects of high concentrations of ionic liquid on GB1 protein structure and dynamics probed by high-resolution magic-angle-spinning NMR spectroscopy. *Biochem. Biophys. Res. Commun.* **2016**, 487, 75–80.
- (13) Brenna, S.; Posset, T.; Furrer, J.; Blümel, J. ¹⁴N NMR and Two-Dimensional Suspension ¹H and ¹³C HRMAS NMR Spectroscopy of Ionic Liquids Immobilized on Silica. *Chem. - Eur. J.* **2006**, 12 (10), 2880–2888.
- (14) Abbott, A. P.; Boothby, D.; Capper, G.; Davies, D. L.; Rasheed, R. K. Deep Eutectic Solvents Formed between Choline Chloride and Carboxylic Acids: Versatile Alternatives to Ionic Liquids. *J. Am. Chem. Soc.* **2004**, 126 (29), 9142–9147.
- (15) Bica, K.; Rodriguez, H.; Gurau, G.; Andreea Cojocaru, O.; Riisager, A.; Fehrmann, R.; Rogers, R. D. Pharmaceutically active ionic liquids with solids handling, enhanced thermal stability, and fast release. *Chem. Commun.* **2012**, 48 (44), 5422–5424.
- (16) O'Neil, M. J. *The Merck index: An encyclopedia of chemicals, drugs, and biological*, 14th ed.; Wiley: 2006.
- (17) Park, H. J.; Prausnitz, M. R. Lidocaine-ibuprofen ionic liquid for dermal anesthesia. *AIChE J.* **2015**, 61 (9), 2732–2738.
- (18) Berton, P.; Di Bona, K. R.; Yancey, D.; Rizvi, S. A. A.; Gray, M.; Gurau, G.; Shamshina, J. L.; Rasco, J. F.; Rogers, R. D. Transdermal Bioavailability in Rats of Lidocaine in the Forms of Ionic Liquids, Salts, and Deep Eutectic. *ACS Med. Chem. Lett.* **2017**, 8 (5), 498–503.
- (19) Metz, G.; Ziliox, M.; Smith, S. O. Towards quantitative CP-MAS NMR. *Solid State Nucl. Magn. Reson.* **1996**, 7 (3), 155–160.
- (20) Fung, B. M.; Khitrin, A. K.; Ermolaev, K. An Improved Broadband Decoupling Sequence for Liquid Crystals and Solids. *J. Magn. Reson.* **2000**, 142 (1), 97–101.
- (21) Marion, D.; Ikura, M.; Tschudin, R.; Bax, A. Rapid recording of 2D NMR spectra without phase cycling. Application to the study of hydrogen exchange in proteins. *J. Magn. Reson. (1969-1992)* **1989**, 85 (2), 393–399.
- (22) Hayashi, S.; Hayamizu, K. Chemical Shift Standards in High-Resolution Solid-State NMR (1) ¹³C, ²⁹Si, and ¹H Nuclei. *Bull. Chem. Soc. Jpn.* **1991**, 64 (2), 685–687.
- (23) Morcombe, C. R.; Zilm, K. W. Chemical shift referencing in MAS solid state NMR. *J. Magn. Reson.* **2003**, 162 (2), 479–486.
- (24) Sarkar, R.; Mainz, A.; Busi, B.; Barbet-Massin, E.; Kranz, M.; Hofmann, T.; Reif, B. Immobilization of soluble protein complexes in MAS solid-state NMR: Sedimentation versus viscosity. *Solid State Nucl. Magn. Reson.* **2016**, 76–77, 7–14.
- (25) Muller, N.; Reiter, R. C. Temperature Dependence of Chemical Shifts of Protons in Hydrogen Bonds. *J. Chem. Phys.* **1965**, 42 (9), 3265–3269.
- (26) Arnold, J. T.; Packard, M. E. Variations in Absolute Chemical Shift of Nuclear Induction Signals of Hydroxyl Groups of Methyl and Ethyl Alcohol. *J. Chem. Phys.* **1951**, 19 (12), 1608–1609.
- (27) Liddel, U.; Ramsey, N. F. Temperature Dependent Magnetic Shielding in Ethyl Alcohol. *J. Chem. Phys.* **1951**, 19 (12), 1608–1608.
- (28) Modig, K.; Halle, B. Proton Magnetic Shielding Tensor in Liquid Water. *J. Am. Chem. Soc.* **2002**, 124 (40), 12031–12041.
- (29) Li, Y.; Jia, Y.; Wang, Z.; Li, X.; Feng, W.; Deng, P.; Yuan, L. An insight into the extraction of transition metal ions by picolinamides associated with intramolecular hydrogen bonding and rotational isomerization. *RSC Adv.* **2014**, 4 (56), 29702–29714.
- (30) Webber, A. L.; Elena, B.; Griffin, J. M.; Yates, J. R.; Pham, T. N.; Mauri, F.; Pickard, C. J.; Gil, A. M.; Stein, R.; Lesage, A.; Emsley, L.; Brown, S. P. Complete ¹H resonance assignment of β-maltose from ¹H-¹H DQ-SQ CRAMPS and ¹H (DQ-DUMBO)-¹³C SQ refocused INEPT 2D solid-state NMR spectra and first principles GIPAW calculations. *Phys. Chem. Chem. Phys.* **2010**, 12 (26), 6970–6983.
- (31) Brown, S. P.; Schnell, I.; Brand, J. D.; Mullen, K.; Spiess, H. W. The competing effects of π-π packing and hydrogen bonding in a hexabenzocoronene carboxylic acid derivative: A ¹H solid-state MAS NMR investigation. *Phys. Chem. Chem. Phys.* **2000**, 2 (8), 1735–1745.
- (32) Dumez, J.; Pickard, C. J. Calculation of NMR chemical shifts in organic solids: Accounting for motional effects. *J. Chem. Phys.* **2009**, 130 (10), 104701.
- (33) Khankari, R. K.; Grant, D. J. W. Pharmaceutical hydrates. *Thermochim. Acta* **1995**, 248, 61–79.
- (34) Tian, F.; Qu, H.; Zimmermann, A.; Munk, T.; Jørgensen, A. C.; Rantanen, J. Factors affecting crystallization of hydrates. *J. Pharm. Pharmacol.* **2010**, 62 (11), 1534–1546.
- (35) Damron, J. T.; Kersten, K. M.; Pandey, M. K.; Mroue, K. H.; Yarava, J. R.; Nishiyama, Y.; Matzger, A. J.; Ramamoorthy, A. Electrostatic Constraints Assessed by ¹H MAS NMR Illuminate Differences in Crystalline Polymorphs. *J. Phys. Chem. Lett.* **2017**, 8 (17), 4253–4257.
- (36) Damron, J. T.; Kersten, K. M.; Pandey, M. K.; Nishiyama, Y.; Matzger, A.; Ramamoorthy, A. Role of Anomalous Water Constraints in the Efficacy of Pharmaceuticals Probed by ¹H Solid-State NMR. *ChemistrySelect* **2017**, 2 (23), 6797–6800.
- (37) Zheng, L.; Fishbein, K. W.; Griffin, R. G.; Herzfeld, J. Two-dimensional solid-state proton NMR and proton exchange. *J. Am. Chem. Soc.* **1993**, 115 (14), 6254–6261.
- (38) Bodet, O.; Goerke, S.; Behl, N. G. R.; Roeloffs, V.; Zaiss, M.; Bachert, P. Amide proton transfer of carnosine in aqueous solution studied in vitro by WEX and CEST experiments. *NMR Biomed.* **2015**, 28 (9), 1097–1103.
- (39) Dai, Y.; van Spronsen, J.; Witkamp, G.-J.; Verpoorte, R.; Choi, Y. H. Natural deep eutectic solvents as new potential media for green technology. *Anal. Chim. Acta* **2013**, 766, 61–68.
- (40) Higashi, K.; Yamamoto, K.; Pandey, M. K.; Mroue, K. H.; Moribe, K.; Yamamoto, K.; Ramamoorthy, A. Insights into Atomic-level Interaction between Mefenamic Acid and Eudragit® EPO in a Supersaturated Solution by High-Resolution Magic-Angle Spinning NMR Spectroscopy. *Mol. Pharmaceutics* **2014**, 11 (1), 351–357.
- (41) Bennett, A. E.; Griffin, R. G.; Ok, J. H.; Vega, S. Chemical shift correlation spectroscopy in rotating solids: Radio frequency-driven dipolar recoupling and longitudinal exchange. *J. Chem. Phys.* **1992**, 96 (11), 8624–8627.
- (42) Pandey, M. K.; Vivekanandan, S.; Yamamoto, K.; Im, S.; Waskell, L.; Ramamoorthy, A. Proton-detected 2D radio frequency driven recoupling solid-state NMR studies on micelle-associated cytochrome-b5. *J. Magn. Reson.* **2014**, 242, 169–179.
- (43) Ramamoorthy, A.; Xu, J. 2D ¹H/¹H RFDR and NOESY NMR Experiments on a Membrane-Bound Antimicrobial Peptide Under Magic Angle Spinning. *J. Phys. Chem. B* **2013**, 117 (22), 6693–6700.
- (44) Kubo, A.; McDowell, C. A. Spectral spin diffusion in polycrystalline solids under magic-angle spinning. *J. Chem. Soc., Faraday Trans. 1* **1988**, 84 (11), 3713–3730.
- (45) Meier, B. H. Polarization transfer and spin diffusion in solid-state NMR. *Adv. Magn. Opt. Reson.* **1994**, 18, 1–116.
- (46) Gabl, S.; Steinhäuser, O.; Weingärtner, H. From Short-Range to Long-Range Intermolecular NOEs in Ionic Liquids: Frequency Does Matter. *Angew. Chem.* **2013**, 125 (35), 9412–9416.
- (47) Heimer, N. E.; Del Sesto, R. E.; Carper, W. R. Evidence for spin diffusion in a ¹H/¹H-NOESY study of imidazolium tetrafluoroborate ionic liquids. *Magn. Reson. Chem.* **2004**, 42 (1), 71–75.
- (48) Harris, R. K. Applications of solid-state NMR to pharmaceutical polymorphism and related matters. *J. Pharm. Pharmacol.* **2007**, 59 (2), 225–239.

(49) Chattah, A. K.; Zhang, R.; Mroue, K. H.; Pfund, L. Y.; Longhi, M. R.; Ramamoorthy, A.; Garnero, C. Investigating Albendazole Desmotropes by Solid-State NMR Spectroscopy. *Mol. Pharmaceutics* **2015**, *12* (3), 731–741.